

Discovering an Invisibly Decaying Higgs at Hadron Colliders

Hooman Davoudiasl,^{1,*} Tao Han,^{1,2,†} and Heather E. Logan^{1,‡}

¹*Department of Physics, University of Wisconsin, Madison, WI 53706*

²*Fermi National Accelerator Laboratory, P.O. Box 500, Batavia, IL 60510*

Abstract

A Higgs boson lighter than $2m_W$ that decays mostly into invisible channels (*e.g.*, dark matter particles) is theoretically well-motivated. We study the prospects for discovery of such an invisible Higgs, h_{inv} , at the LHC and the Tevatron in three production modes: (1) in association with a Z , (2) through Weak Boson Fusion (WBF), and (3) accompanied by a jet. In the $Z + h_{inv}$ channel, we show that the LHC can yield a discovery signal above 5σ with 10 fb^{-1} of integrated luminosity for a Higgs mass of 120 GeV. With 30 fb^{-1} the discovery reach extends up to a Higgs mass of 160 GeV. We also study the extraction of the h_{inv} mass from production cross sections at the LHC, and find that combining WBF and $Z + h_{inv}$ allows a relatively model-independent determination of the h_{inv} mass with an uncertainty of 35–50 GeV (15–20 GeV) with 10 (100) fb^{-1} . At the Tevatron, a 3σ observation of a 120 GeV h_{inv} in any single channel is not possible with less than 12 fb^{-1} per detector. However, we show that combining the signal from WBF with the previously-studied $Z + h_{inv}$ channel allows a 3σ observation of h_{inv} with 7 fb^{-1} per detector. Because of overwhelming irreducible backgrounds, $h_{inv} + j$ is not a useful search channel at either the Tevatron or the LHC, despite the larger production rate.

*Electronic address: hooman@physics.wisc.edu

†Electronic address: than@physics.wisc.edu

‡Electronic address: logan@physics.wisc.edu

I. INTRODUCTION

The Higgs particle is the only missing part of the highly successful Standard Model (SM) of particle physics. The current experimental data from direct searches [1] and electroweak precision measurements [2] point to a Higgs mass in the range $114 \text{ GeV} < m_h \lesssim 250 \text{ GeV}$. Thus, if the Higgs exists the Tevatron might detect it in the next several years and the LHC is expected to discover it.

Most analyses assume that the Higgs will predominantly decay into detectable SM fields. However, this may not be a good assumption if there are new weakly interacting particles with mass less than half the Higgs mass that couple to the Higgs with $\mathcal{O}(1)$ strength. In this case, if $m_h < 160 \text{ GeV} \simeq 2 m_W$ so that the Higgs partial width into SM particles is very small, the Higgs will decay predominantly into the new weakly interacting particles. In particular, if these new weakly interacting particles are neutral and stable, the Higgs will decay *invisibly*. There are many models in which this situation is realized, such as the Minimal Supersymmetric Standard Model (MSSM, with Higgs decays to lightest neutralinos), models with extra dimensions (with Higgs decays to Kaluza-Klein neutrinos [3]), and Majoron models [4]. An invisible Higgs is also quite generic in minimal models of dark matter containing a stable singlet scalar [5, 6, 7]. From a phenomenological point of view, the existence of dark matter in the universe provides compelling evidence for stable neutral particles with weak scale masses and couplings. Given unsuppressed couplings and suitable masses, the Higgs would decay nearly exclusively into these particles and become invisible in collider experiments. The combined LEP experimental bound on the mass of an invisibly-decaying Higgs boson is 114.4 GeV at 95% confidence level [8].

In this paper, we study the discovery potential for the invisible Higgs h_{inv} at the LHC and the Tevatron. We focus on three production channels: $Z + h_{inv}$, $h_{inv} + jj$ in Weak Boson Fusion (WBF), and $h_{inv} + j$ in gluon fusion. There have been a number of similar studies in the past [9, 10, 11, 12, 13, 14, 15, 16]. We also examine the prospects for determining the mass of the invisible Higgs from production cross sections at the LHC. We will show that the $Z + h_{inv}$ channel gives a surprisingly good handle on the Higgs mass given 100 fb^{-1} of integrated luminosity. We will also show how the $Z + h_{inv}$ and WBF channels can be combined at the LHC to remove model assumptions from the Higgs mass extraction.

Discovery of the Higgs in the $Z + h_{inv}$ channel was studied for the LHC in Refs. [11,

14]. This channel was also analyzed for the Tevatron in Ref. [12]. In Ref. [11], the Z +jet background at the LHC was found to diminish the significance of the signal considerably, and the electroweak backgrounds coming from WW and ZW final states were ignored. We will show that, with the kinematic acceptance and the cuts we adopt, the prospects for the discovery of the invisible Higgs in $Z + h_{inv}$ at the LHC are brighter than presented in Ref. [11], even with the WW and ZW backgrounds included. Our results are consistent with those of Ref. [14].

WBF production of the invisible Higgs was studied for the LHC in Ref. [13], which showed that WBF can provide significant signals for invisible Higgs discovery, even at low luminosity. Here, we will use their approach to show that WBF contributes significantly to the observation of h_{inv} at the Tevatron. Even though a 3σ observation of a 120 GeV h_{inv} in any single channel at the Tevatron is not possible with less than 12 fb^{-1} per detector, one can enhance the significance of the signal by combining data from various channels. At the Tevatron, an important production mode is $Z + h_{inv}$ [12] and yields a somewhat larger significance than the WBF channel that we study. Combining these two channels and data from two Tevatron detectors, we show that a 3σ observation of h_{inv} with $m_h = 120 \text{ GeV}$ can be obtained with 7 fb^{-1} of integrated luminosity per detector.

In the case of $h_{inv} + j$, we study the size of the irreducible background generated by $Z(\rightarrow \nu\bar{\nu}) + j$. Although $h_{inv} + j$ is the leading triggerable production cross section for h_{inv} at both the LHC and the Tevatron [17], the $Z(\rightarrow \nu\bar{\nu}) + j$ background is so large that we conclude that this channel cannot help to discover h_{inv} .

In the next section, we consider the $Z + h_{inv}$ production mode at the LHC, present our kinematic cuts, and examine various backgrounds. We also discuss the Higgs mass extraction from cross section measurements. In Sec. III, we consider h_{inv} production via WBF at the Tevatron. The contribution of the $h_{inv} + j$ mode at both the Tevatron and the LHC is discussed in Sec. IV. Section V contains a discussion of our results and other concluding remarks.

II. ASSOCIATED $Z + h_{inv}$ PRODUCTION AT THE LHC

In this section, we consider the production of h_{inv} in association with a Z boson

$$pp \rightarrow Z(\rightarrow \ell^+ \ell^-) + h_{inv} ; \quad \ell = e, \mu, \quad (1)$$

at the LHC. This process was previously studied for the LHC in Refs. [11, 14]. We update and refine the analysis of Ref. [11] by taking into account sources of background not included in that study and considering a wider acceptance range for the leptons. In our analysis, we assume that the Higgs decays 100% of the time to invisible final states, and that the production cross section is the same as in the SM. Our results can be easily scaled for other invisible branching fractions or non-SM production cross sections. Detection of the $Z + h_{inv}$ signal at the Tevatron has been previously studied in Ref. [12] and we will later mention their results for comparison. We will comment on the effects of departure from the assumption of a completely invisible Higgs in Sec. V.

1. Signal for h_{inv}

As the signal is $\ell^+\ell^-\cancel{p}_T$, the most significant sources of background are

$$Z(\rightarrow \ell^+\ell^-)Z(\rightarrow \nu\bar{\nu}), \quad W^+(\rightarrow \ell^+\nu)W^-(\rightarrow \ell^-\bar{\nu}), \quad Z(\rightarrow \ell^+\ell^-)W(\rightarrow \ell\nu), \quad (2)$$

(with the lepton from the W decay in ZW missed) and $Z + \text{jets}$ final states with fake \cancel{p}_T [11, 12]. We simulate the signal and the first three backgrounds for the LHC using Madgraph [18].

We start with the following ‘‘minimal cuts’’:

$$p_T(\ell^\pm) > 10 \text{ GeV}, \quad |\eta(\ell^\pm)| < 2.5, \quad \Delta R(\ell^+\ell^-) > 0.4, \quad (3)$$

where η denotes pseudo-rapidity and ΔR is the separation between the two particles in the detector, $\Delta R \equiv \sqrt{(\Delta\eta)^2 + (\Delta\phi)^2}$; ϕ is the azimuthal angle. The electromagnetic calorimeter at both ATLAS [19] and CMS [20] covers the range $|\eta| < 3$; however, the electron trigger covers only $|\eta| < 2.5$ (2.6) at ATLAS (CMS). The pseudo-rapidity acceptance for dielectrons could be expanded by requiring only one electron within $|\eta| < 2.5$ and the other within $|\eta| < 3$. Meanwhile, the muon trigger covers $|\eta| < 2.2$ (2.1) at ATLAS (CMS), with muon identification and momentum measurement out to $|\eta| < 2.4$. We require $|\eta(\ell^\pm)| < 2.5$ for both leptons, so that the larger acceptance for dielectron events compensates the smaller acceptance for dimuon events.

Because we will cut on the invariant mass of the dilepton pair to keep only events in which the dileptons reconstruct to the Z mass, we imitate the effects of LHC detector resolution

by smearing the electron momenta according to

$$\Delta E/E = \frac{0.1}{\sqrt{E \text{ (GeV)}}} \oplus 0.5\%, \quad (4)$$

with the two contributions added in quadrature. This smearing has a negligible effect on our results. We have thus applied the same smearing to the final state with muons.

The WW background can be largely eliminated by requiring that the $\ell^+\ell^-$ invariant mass $m_{\ell^+\ell^-}$ is close to m_Z :

$$|m_{\ell^+\ell^-} - m_Z| < 10 \text{ GeV}. \quad (5)$$

Also, the ℓ^+ and ℓ^- from two different parent W bosons tend to be more back-to-back than the leptons in the signal. We therefore impose an azimuthal angle cut on the lepton pair,

$$\Delta\phi_{\ell^+\ell^-} < 2.5 \text{ or } 143^\circ. \quad (6)$$

This cut also eliminates Drell-Yan backgrounds with fake \cancel{p}_T caused by mismeasurement of the lepton energies.

Our third cut is on \cancel{p}_T . The number of $\ell^+\ell^- \cancel{p}_T$ signal events typically falls more slowly with \cancel{p}_T than those of the ZZ or WW backgrounds, as shown in Fig. 1. The \cancel{p}_T of the WW background is typically quite low because the \cancel{p}_T comes from the two neutrinos emitted independently in the two W decays. The typical \cancel{p}_T of the ZZ background is somewhat larger, but still smaller than that of the signal. This is because ZZ production comes from t -channel diagrams in which the Z decaying to neutrinos itself tends to carry less p_T than the h_{inv} produced via s -channel Higgsstrahlung. As a result, the signal falls off with increasing \cancel{p}_T at a slower rate than the ZZ background, as reflected by the increase in S/B as \cancel{p}_T gets larger, in Table II. The \cancel{p}_T distribution of the signal is also sensitive to the Higgs mass; it falls off more slowly with increasing \cancel{p}_T , as m_h gets larger. Thus a fit to the \cancel{p}_T distribution can in principle give some limited sensitivity to the Higgs mass. We note that the measurement of \cancel{p}_T at hadron colliders suffers from a lot of systematic effects. However, for the process with $Z \rightarrow \ell^+\ell^-$, the \cancel{p}_T spectrum is largely determined by the well-measured lepton momenta, which can make the systematic uncertainty minimal.

The final state $Z(\rightarrow \ell^+\ell^-)W(\rightarrow \ell\nu)$, where the lepton from the W decay is missed, can be a potential background. However, the probability of missing the lepton from the W decay is small given the kinematic coverage at the LHC. To reduce this background, we veto events

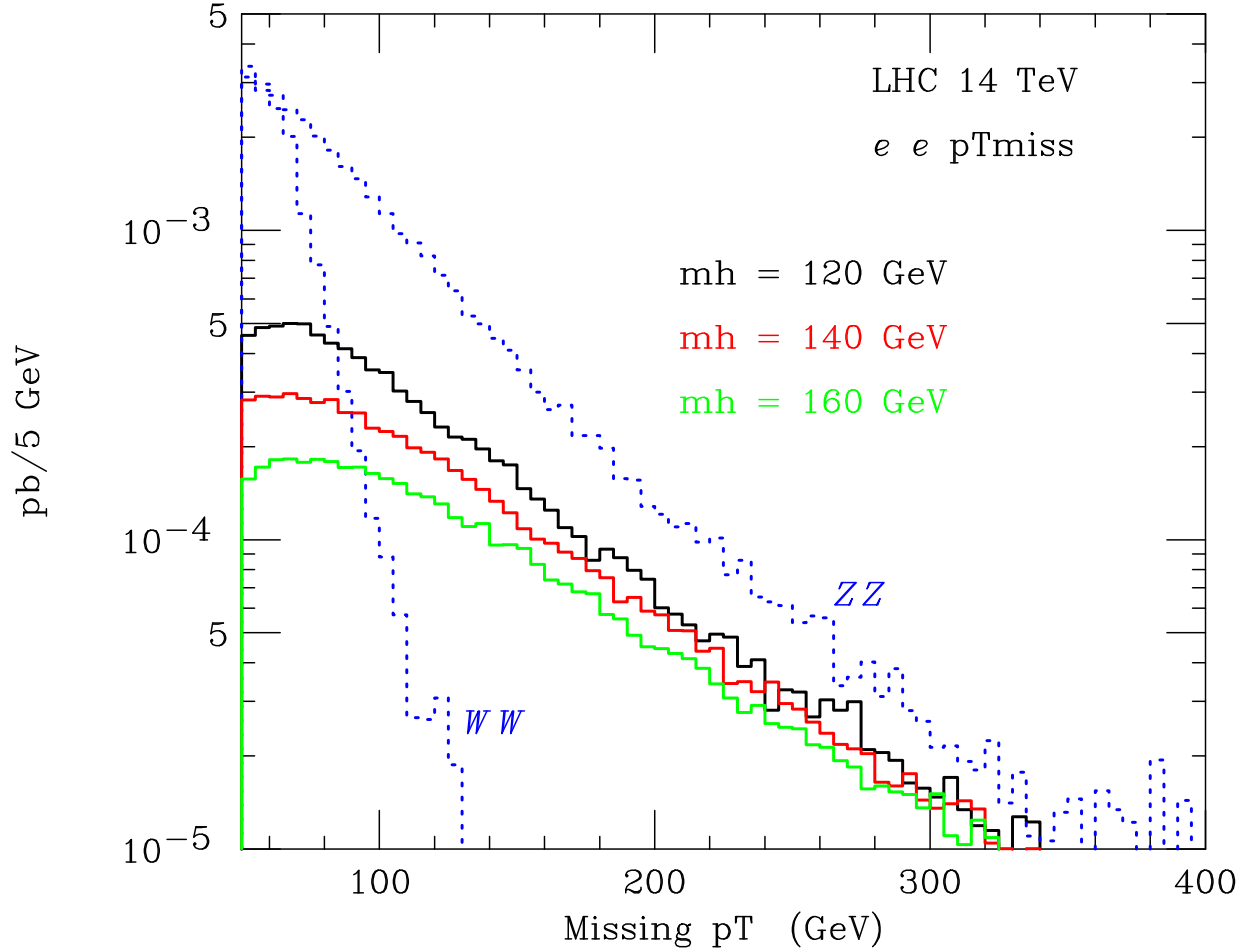


FIG. 1: Missing p_T distribution for $Z(\rightarrow e^+e^-) + h_{inv}$ signal (solid lines, with $m_h = 120, 140$ and 160 GeV top to bottom) and backgrounds from WW and ZZ (dotted lines) at the LHC, after applying the cuts in Eqs. (3), (5) and (6).

with a third isolated electron with

$$p_T > 10 \text{ GeV}, \quad |\eta| < 3.0. \quad (7)$$

For simplicity, we apply the same veto to W decays to muons or taus. This veto reduces the $Z + W$ background to the level of 5–10 fb, so that it has little effect on the significance of the signal.

We also include the background from Z +jets with fake \cancel{p}_T . As shown in Ref. [11], events of the type Z +jets can constitute a significant background due to jet energy mismeasurements resulting in fake \cancel{p}_T , or when one or more jets are emitted outside the fiducial region of the detector and are therefore missed. The majority of those events can be eliminated

by applying a jet veto, but those in which the jet(s) are soft and/or escape down the beampipe can fake $Z + \cancel{p}_T$ events. A simulation of the latter requires simulating the detector effects, which is beyond the scope of our analysis. Instead, we adopt the results for this background from Ref. [11]. We note that these authors impose a lepton isolation cone angle of $\Delta R(\ell^+\ell^-) > 0.7$ radians, which results in a smaller acceptance than our cuts in Eq. (3). A comparison of our signal and ZZ background cross sections in Table I for $\cancel{p}_T > 65$ GeV with those in the last entry of Table I in Ref. [11] shows that our larger acceptance results in a factor of ~ 1.6 larger cross sections.

In Ref. [11], with the cuts $\cancel{p}_T > 65$ GeV and $|m_{\ell^+\ell^-} - m_Z| < 5$ GeV and vetoing jets with $p_T(j) > 45$ GeV and $|\eta(j)| < 4.7$, the background cross section coming from Z +jets is 13.91 fb, combining e^+e^- and $\mu^+\mu^-$ final states. Changing the Z -mass cut from $|m_{\ell^+\ell^-} - m_Z| < 5$ GeV to 10 GeV as assumed in our study does not significantly affect the cross sections of processes with the $\ell^+\ell^-$ coming from a real Z boson. Rescaling this result by a factor of 1.6 to take into account our larger lepton acceptance as discussed above, we thus expect a Z +jets background cross section of 22 fb for $\cancel{p}_T > 65$ GeV. Reference [11] also found (for a different choice of $\eta(j)$ acceptance) that increasing the \cancel{p}_T cut from 65 GeV to 75 GeV reduces the Z +jets background by a factor of about 3.4. We thus estimate a Z +jets background cross section of about 9 fb for $\cancel{p}_T > 75$ GeV with our cuts. We note that this estimate is quite likely a conservative one, since we have only used a factor of ~ 2.5 reduction of the background in extrapolating from $\cancel{p}_T > 65$ GeV to $\cancel{p}_T > 75$ GeV. In addition, at the LHC, whereas the pseudo-rapidity acceptance of the calorimeter in the CMS detector is ± 4.7 [20], that of the ATLAS detector is ± 4.9 [19] which helps in the suppression of the fake \cancel{p}_T background.

At this point, we note that there are other potentially large sources of background that need to be addressed [12]. The background events from $Z^* \rightarrow \tau^+\tau^- \rightarrow \ell^+\ell^- \cancel{p}_T$ are efficiently suppressed by our Z -mass cut on $m_{\ell^+\ell^-}$, the \cancel{p}_T cut, and the cut on $\Delta\phi_{\ell^+\ell^-}$ that requires that the leptons are not back-to-back. This can be seen from Table 2 in Ref. [14], where it is shown that, after cuts similar to those we use, the resulting background from a single Z is basically absent for the ZH production channel. The same conclusion is reached for the W + jet background in the ZH channel, in Table 2 of Ref. [14]. Hence, fake events from $W(\rightarrow \ell\nu)$ +jet, where the jet is misidentified as a lepton of the appropriate charge and flavor, are also ignored in our analysis.

Our results for the background and signal cross sections are tabulated in Table I. The corresponding signal to background ratio, S/B , and significance, S/\sqrt{B} , are tabulated in Table II. The numbers given in parentheses represent the significance obtained including our estimated Z +jets background discussed above. To be cautious, we only consider this background for the cases with $\cancel{p}_T > 65$ GeV and $\cancel{p}_T > 75$ GeV, which were studied in Ref. [11], and refrain from extrapolating to other \cancel{p}_T cut values. We see from Table II that a $> 5\sigma$ discovery can be obtained for $m_h = 120$ GeV with 10 fb^{-1} of integrated luminosity, even with our conservative estimate for the Z +jets background for $\cancel{p}_T > 75$ GeV.

\cancel{p}_T cut	B				S($Z + h_{inv}$)		
	B(ZZ)	B(WW)	B(ZW)	B($Z + j$)*	$m_h = 120$	140	160 GeV
65 GeV	48.0 fb	10.6 fb	10.2 fb	22 fb	14.8 fb	10.8 fb	7.9 fb
75 GeV	38.5 fb	4.3 fb	7.4 fb	9 fb	12.8 fb	9.4 fb	7.0 fb
85 GeV	30.9 fb	1.8 fb	5.5 fb		11.1 fb	8.3 fb	6.3 fb
100 GeV	22.1 fb	0.6 fb	3.6 fb		8.7 fb	6.8 fb	5.3 fb

TABLE I: Background and signal cross sections for associated $Z(\rightarrow \ell^+\ell^-) + h_{inv}$ production at the LHC, combining the ee and $\mu\mu$ channels. *Estimated from Ref. [11] (see text for details).

\cancel{p}_T cut	$m_h = 120$ GeV			$m_h = 140$ GeV	$m_h = 160$ GeV
	S/B	S/\sqrt{B} (10 fb^{-1})	S/\sqrt{B} (30 fb^{-1})	S/\sqrt{B} (30 fb^{-1})	S/\sqrt{B} (30 fb^{-1})
65 GeV	0.22 (0.16)	5.6 (4.9)	9.8 (8.5)	7.1 (6.2)	5.2 (4.5)
75 GeV	0.25 (0.22)	5.7 (5.3)	9.9 (9.1)	7.3 (6.7)	5.4 (5.0)
85 GeV	0.29	5.7	9.8	7.4	5.6
100 GeV	0.33	5.4	9.3	7.3	5.7

TABLE II: Signal significance for associated $Z(\rightarrow \ell^+\ell^-) + h_{inv}$ production at the LHC, combining the ee and $\mu\mu$ channels. The numbers in the parentheses include the estimated Z +jets background discussed in the text.

Reference [11] finds a 14σ signal for h_{inv} at the LHC with 100 fb^{-1} and $\cancel{p}_T > 65$ GeV, with the rest of their cuts as mentioned above. Rescaling this result for 10 fb^{-1} yields a 4.4σ signal, somewhat more pessimistic than our result for the signal significance for $\cancel{p}_T > 65$ GeV

in Table II. Our larger significance for $\cancel{p}_T > 65$ GeV is due solely to our larger lepton acceptance: we accept roughly 1.6 times as many events as the study in Ref. [11]. Rescaling their results by $\sqrt{1.6}$ to account for this larger acceptance, their significance becomes 5.6σ . Our significance for $\cancel{p}_T > 65$ GeV in Table II is lower than 5.6σ because we have included the WW and ZW backgrounds, which were neglected in Ref. [11]. We also found that the signal significance can be improved somewhat by increasing the \cancel{p}_T cut above 65 GeV; the optimum cut appears to be roughly 75–85 GeV.

Our results are in qualitative agreement with the study of Godbole et al. in Ref. [14], which included hadronization of the $Z + h_{inv}$ signal and backgrounds using Pythia/Herwig. For the same cut on \cancel{p}_T of 100 GeV, Ref. [14] found a signal cross section smaller by about 30% than our result, and a total background cross section (dominated by ZZ production) smaller by about 20%. We expect that this reduction in both the signal and background cross sections is due to events being rejected by the jet veto imposed in Ref. [14] after including QCD initial-state radiation. The 30% reduction in signal cross section can be compensated [12] by the known NLO QCD K-factor for $Z + h$ at LHC of about 1.3 [21], yielding a signal cross section consistent with our result. Similarly, the reduction in the dominant ZZ background can be compensated by the known NLO QCD K-factor for ZZ at LHC of about 1.2 [22], yielding a background cross section consistent with our result. We have not explicitly included any K-factors in our signal or background cross section calculations, with the expectation of some reduction due to the jet vetoing requirement.

For comparison, a 3σ observation of h_{inv} at the same mass at the Tevatron will require 26 fb^{-1} , and with 30 fb^{-1} it is possible to observe a 125 GeV h_{inv} at the 3σ level [12]. However, at the LHC, with 30 fb^{-1} and given our conservative estimate of Z +jets background, a 5σ discovery or better is possible up to $m_h = 160$ GeV, as shown in Table II. For higher Higgs masses, the $h \rightarrow WW$ decay goes on-shell, increasing the Higgs width significantly. The decay to WW will then most likely compete with the invisible decay mode, resulting in a partly-visible Higgs.

The $Z + h_{inv}$ channel can thus be used at the LHC for $m_h \lesssim 160$ GeV to supplement the WBF channel [13], which has higher significance. However, we would like to emphasize that the \cancel{p}_T measurements in the process $\ell^+\ell^-\cancel{p}_T$ that we studied here are largely determined by $p_T(\ell\ell)$, and the distribution will suffer much less from systematic uncertainties compared to the WBF where \cancel{p}_T is determined mainly from the forward jets.

2. Higgs boson mass

The $Z + h_{inv}$ channel may also provide an interesting handle on the Higgs boson mass, as follows. The mass of an invisibly-decaying Higgs boson obviously cannot be reconstructed from the Higgs decay products. Unless the Higgs is also observed in a visible channel, our only chance of determining the Higgs mass comes from the m_h dependence of the production process. Extracting m_h from the production cross section requires the assumption that the production couplings are the same as in the SM. (Non-observation of the Higgs in any visible final state implies that the invisible branching fraction is close to 100%.)

The Higgs mass extraction from measurements of the production cross sections in $Z + h_{inv}$ and WBF are shown in Tables III and IV, respectively. There are two sources of uncertainty in the signal: statistical and from background normalization. The statistical uncertainty is $\Delta\sigma_S/\sigma_S = \sqrt{S+B}/S$. We estimate the total background normalization uncertainty for $Z + h_{inv}$ to be the same size as that of the dominant process involving $Z \rightarrow \nu\nu$: $\Delta B/B = \Delta B(ZZ)/B(ZZ)$. We assume that this background can be measured via the corresponding channels in which $Z \rightarrow \ell^+\ell^-$ and take the uncertainty to be the statistical uncertainty on the $Z \rightarrow \ell^+\ell^-$ rate: $\Delta B(ZZ)/B(ZZ) \simeq 7.1\%$ (2.2%), for an integrated luminosity of 10 (100) fb^{-1} . In Tables III and IV we quote the resulting uncertainty on the signal cross section, given by $\Delta\sigma_S/\sigma_S = (B/S) \times \Delta B/B$. The total uncertainty $[\Delta\sigma_S/\sigma_S]_{tot}$, presented in Tables III and IV, is then the sum, in quadrature, of the statistical and background uncertainties, as well as other uncertainties that may exist. We then have $\Delta m_h = (1/\rho)[\Delta\sigma_S/\sigma_S]_{tot}$; ρ is defined in Tables III and IV.

The cross section for $Z + h_{inv}$ production falls quickly with increasing m_h due to the s -channel propagator suppression. This is in contrast to the WBF production, which provides a $> 5\sigma$ signal up to $m_h \simeq 480$ GeV with 10 fb^{-1} if the Higgs decays completely invisibly [13]. Thus, while the statistics are much better on the WBF measurement than on $Z + h_{inv}$, the systematic uncertainties hurt WBF more because $(d\sigma_S/dm_h)/\sigma_S$ is much smaller for WBF than for $Z + h_{inv}$. The $Z + h_{inv}$ cross section is therefore more sensitive to the Higgs mass than the WBF cross section.

More importantly, however, taking the ratio of the $Z + h_{inv}$ and WBF cross sections allows for a more model-independent determination of the Higgs mass. This is due to the fact that the production couplings in $Z + h_{inv}$ (hZZ) and in WBF (contributions from

m_h (GeV)	120	140	160
$\rho = (d\sigma_S/dm_h)/\sigma_S$ (1/GeV)	-0.013	-0.015	-0.017
Statistical uncert.	21% (6.6%)	28% (8.8%)	37% (12%)
Background normalization uncert.	33% (10%)	45% (14%)	60% (19%)
Total uncert.	40% (16%)	53% (19%)	71% (24%)
Δm_h (GeV)	30 (12)	35 (12)	41 (14)

TABLE III: Higgs mass determination from $Z + h_{inv}$ with 10 (100) fb^{-1} , assuming Standard Model production cross section and 100% invisible decays. The signal and background cross sections were taken from Table I for $\cancel{p}_T > 75$ GeV. The total uncertainty includes a theoretical uncertainty on the signal cross section from QCD and PDF uncertainties of 7% [23] and an estimated lepton reconstruction efficiency uncertainty of 4% (2% per lepton) and luminosity normalization uncertainty of 5% [24].

m_h (GeV)	120	130	150	200
$\rho = (d\sigma_S/dm_h)/\sigma_S$ (1/GeV)	-0.0026	-0.0026	-0.0028	-0.0029
Statistical uncert.	5.3% (1.7%)	5.4% (1.7%)	5.7% (1.8%)	6.4% (2.0%)
Background normalization uncert.	5.2% (2.1%)	5.3% (2.1%)	5.6% (2.2%)	6.5% (2.6%)
Total uncert.	11% (8.6%)	11% (8.6%)	11% (8.6%)	12% (8.8%)
Δm_h (GeV)	42 (32)	42 (33)	41 (31)	42 (30)

TABLE IV: Higgs mass determination from $\text{WBF} \rightarrow h_{inv}$ with 10 (100) fb^{-1} , assuming Standard Model production cross section and 100% invisible decays. The background and signal cross sections were taken from Tables II and III, respectively, of Ref. [13], and include a central jet veto. The total uncertainty includes a theoretical uncertainty from QCD and PDF uncertainties of 4% [25], and an estimated uncertainty on the efficiency of the WBF jet tag and central jet veto of 5% and luminosity normalization uncertainty of 5% [24].

hWW and hZZ) are related by custodial $\text{SU}(2)$ symmetry in any model containing only Higgs doublets and/or singlets. The production couplings thus drop out of the ratio of rates in this wide class of models (which includes the MSSM, multi-Higgs-doublet models, and models of singlet scalar dark matter), leaving dependence only on the Higgs mass. The

m_h (GeV)	120	140	160
$r = \sigma_S(Zh)/\sigma_S(\text{WBF})$	0.132	0.102	0.0807
$(dr/dm_h)/r$ (1/GeV)	-0.011	-0.013	-0.013
Total uncert., $\Delta r/r$	41% (16%)	54% (20%)	72% (25%)
Δm_h (GeV)	36 (14)	43 (16)	53 (18)

TABLE V: Higgs mass determination from the ratio method discussed in the text, with 10 (100) fb^{-1} . The event rates for WBF were interpolated linearly for Higgs masses of 140 and 160 GeV, which were not given explicitly in Ref. [13]. Statistical uncertainties were obtained assuming SM signal rates. The total uncertainty includes theoretical uncertainties from QCD and PDF uncertainties of 7% for $Z + h_{inv}$ [23] and 4% for WBF [25], and estimated uncertainties on the lepton reconstruction efficiency in $Z + h_{inv}$ of 4% (2% per lepton) and on the efficiency of the WBF jet tag and central jet veto of 5% [24]. The luminosity normalization uncertainty cancels out in the ratio of cross sections and is therefore not included.

resulting Higgs mass extraction is illustrated in Table V. Assuming SM event rates for the statistical uncertainties, we find that the Higgs mass can be extracted with an uncertainty of 35–50 GeV (15–20 GeV) with 10 (100) fb^{-1} of integrated luminosity. The ratio method also allows a test of the SM cross section assumption by checking the consistency of the m_h determinations from the $Z + h_{inv}$ and WBF cross sections alone with the m_h value extracted from the ratio method. Furthermore, observation of the invisibly-decaying Higgs in WBF but not in $Z + h_{inv}$ allows one to set a lower limit on m_h in this class of models.

III. PRODUCTION OF h_{inv} VIA WBF AT THE TEVATRON

WBF provides a significant Higgs production mechanism at the LHC and is a promising channel for studying Higgs couplings to weak bosons [26, 27, 28]. Reference [13] studied h_{inv} production in WBF at the LHC and concluded that with only 10 fb^{-1} of integrated luminosity, h_{inv} can be detected at the $\geq 5\sigma$ level up to $m_h \simeq 480$ GeV. They also showed that the invisible branching fraction of a 120 GeV Higgs can be constrained at the 95% confidence level to be less than 13% if no signal is seen in the $\text{WBF} \rightarrow h_{inv}$ channel, again with 10 fb^{-1} .

The kinematic requirements for suppressing the backgrounds rely on the large energy and rapidity of the forward tagging jets characteristic of WBF at the LHC, together with the large rapidity coverage of the LHC detectors. However, given the more limited kinematic range and rapidity coverage at the Tevatron, it is not immediately clear whether implementing the same search strategy will yield a useful signal for h_{inv} . In the following, we will show that the WBF production mode will indeed have a significant impact on the prospects for the observation of h_{inv} at the Tevatron, before data from the LHC becomes available.

The signal here is $\cancel{p}_T + 2j$. A large background comes from $Z(\rightarrow \nu\bar{\nu}) + 2j$ with the jets produced via QCD. A smaller, but less reducible, background comes from $Z(\rightarrow \nu\bar{\nu}) + 2j$ in which the Z is produced by WBF and the jets have kinematics similar to that of the signal. In addition, there are backgrounds from $W(\rightarrow \ell\nu) + 2j$, in which the lepton from the W decay is missed, and QCD backgrounds with fake \cancel{p}_T from missed jets in multi-jet events and jet energy mismeasurements in di-jet events.

We generate the signal, $h_{inv} + 2j$, the QCD and electroweak backgrounds with $Z(\rightarrow \nu\bar{\nu}) + 2j$, and the QCD background with $W(\rightarrow \ell\nu) + 2j$ for the Tevatron using Madgraph [18]. We start with the following “minimal cuts”:

$$p_T(j) > 10 \text{ GeV}, \quad |\eta(j)| < 3.0, \quad \Delta R(jj) > 0.4, \quad \cancel{p}_T > 90 \text{ GeV}. \quad (8)$$

The $\cancel{p}_T > 90 \text{ GeV}$ requirement provides a trigger. We take the calorimeter pseudo-rapidity coverage from, *e.g.*, Ref. [29].

In WBF events, the two jets come from the initial partons, which are at high energy and are not deflected very much by the interaction. To separate the signal from the backgrounds, we thus impose “WBF cuts”: we require that the two jets reconstruct to a large invariant mass,

$$m_{jj} > 320, 340, 360, 400 \text{ GeV}, \quad (9)$$

and are separated by a large rapidity gap,

$$\Delta\eta_{jj} > 2.8. \quad (10)$$

These two cuts eliminate most of the QCD $Z + 2j$ and $W + 2j$ backgrounds, in which the jets tend to be softer and have a smaller rapidity gap, while preserving a significant fraction of the WBF signal.

To reduce the $W + 2j$ background further, we apply a lepton veto. We veto events that contain an isolated electron with [30]

$$p_T(\ell) > 8 \text{ GeV}, \quad |\eta(\ell)| < 3.0. \quad (11)$$

For simplicity, we apply the same veto to W decays to muons or taus. Loosening the veto requirements to $p_T(\ell) > 10 \text{ GeV}$, $|\eta(\ell)| < 2.0$ increases the $W + 2j$ background by about a factor of two.

Background can also come from QCD multi-jet events with fake \cancel{p}_T due to mismeasurement of jets and jet activity escaping down the beampipe. We follow the techniques of a CDF study of $\cancel{p}_T + 2j$ [31] to deal with this background. First we require that the \cancel{p}_T not be aligned with either of the jets:

$$\Delta\phi(j, \cancel{p}_T) > 30^\circ. \quad (12)$$

This eliminates backgrounds containing fake \cancel{p}_T due to jet energy mismeasurement in two-jet events.

The remaining QCD $jj\cancel{p}_T$ background with fake \cancel{p}_T was simulated in Ref. [31] for various minimum \cancel{p}_T cuts. The kinematic cuts on the jets used in Ref. [31] were different than ours: Ref. [31] required $E_T(j_1) > 40 \text{ GeV}$, $E_T(j_2) > 25 \text{ GeV}$, and $|\eta(j_1)|, |\eta(j_2)| < 1$. They allowed a third jet with $E_T > 15 \text{ GeV}$ and $|\eta| < 2.5$, and vetoed events with any additional jets with $E_T > 15 \text{ GeV}$ and $|\eta| < 3.6$. In addition to requiring that the \cancel{p}_T not be aligned with either of the jets, Eq. (12), they required that the two central jets not be back-to-back, $\Delta\phi(j_1, j_2) < 165^\circ$, and that the \cancel{p}_T not be antiparallel to the leading jet, $\Delta\phi(j_1, \cancel{p}_T) < 165^\circ$, in order to eliminate backgrounds with fake \cancel{p}_T from jet energy mismeasurements. For $\cancel{p}_T > 90 \text{ GeV}$, Ref. [31] found a QCD $jj\cancel{p}_T$ background with fake \cancel{p}_T of about 5 fb.

The study in Ref. [31] considers jets in the central region, $|\eta| < 1$, in contrast to our cuts in Eqs. (8) and (10). However, since our cut on the dijet invariant mass, $m_{jj} > 320 \text{ GeV}$ or higher, requires much more visible energy in the jets than the CDF study does, we expect that the QCD background with fake \cancel{p}_T found in Ref. [31] represents a *conservative upper limit* for our cuts. A quantitative estimate of the dijet background with fake \cancel{p}_T would require simulating the detector effects, which is beyond the scope of our analysis.

In Table VI we show results for signal and background cross sections for the m_{jj} cuts given in Eq. (9). In Table VII we show the resulting signal-to-background ratio and significance for 10 fb^{-1} .

m_{jj} cut	$S(h_{inv} + 2j)$	$B(Z + 2j, \text{QCD})$	$B(Z + 2j, \text{EW})$	$B(W + 2j, \text{QCD})$
320 GeV	4.1 fb	55 fb	1.7 fb	7 fb
340 GeV	3.6 fb	43 fb	1.6 fb	5 fb
360 GeV	3.2 fb	34 fb	1.4 fb	5 fb
400 GeV	2.4 fb	21 fb	1.2 fb	2 fb

TABLE VI: Signal and background cross sections for $h_{inv} + 2j$ at Tevatron Run 2, for $m_h = 120$ GeV. The statistical uncertainty on $B(Z + 2j, \text{QCD})$ after cuts is roughly 10% due to our limited Monte Carlo sample. There is an additional background from QCD with fake \cancel{p}_T which is taken from Ref. [31] to be 5 fb; this represents a conservative overestimate of the fake \cancel{p}_T background.

m_{jj} cut	S (10 fb $^{-1}$)	S/B	S/ \sqrt{B} (10 fb $^{-1}$)
320 GeV	41 evts	0.060	1.6
340 GeV	36 evts	0.066	1.5
360 GeV	32 evts	0.070	1.5
400 GeV	24 evts	0.082	1.4

TABLE VII: Number of signal events, signal-to-background ratio, and significance for $h_{inv} + 2j$ at Tevatron Run 2, for $m_h = 120$ GeV. We include the background from QCD with fake \cancel{p}_T of 5 fb [31] in S/B and S/ \sqrt{B} .

From the numbers given in Table VII it is clear that even with 10^{-1} fb of integrated luminosity, the significance is below 2σ . We find a signal significance of about 1.6σ with 10 fb $^{-1}$ of luminosity at one Tevatron detector. This significance is not much less than that found in Ref. [12] for $Z + h_{inv}$ at the Tevatron, namely 1.9σ with 10 fb $^{-1}$ for $m_h = 120$ GeV. Neither of these channels alone is sufficient to provide an observation of h_{inv} : combining data from both Tevatron detectors, a 3σ observation would require at least 12 fb $^{-1}$ in the $Z + h_{inv}$ channel, or 18 fb $^{-1}$ in the WBF channel. However, by combining these two channels, we find that a 3σ observation of h_{inv} is possible with 7 fb $^{-1}$ per detector, if the background can be determined to better than 10%. Thus, WBF provides an important second channel that brings an observation of h_{inv} into the realm of possibility at the Tevatron before the results of the LHC become available. Here, we note that there may be other production channels, such as $gg \rightarrow h_{inv}jj$, that could contribute to the signal, even after the WBF cuts

we have outlined. However, this could only enhance h_{inv} production, making our results for the WBF channel a lower bound on the number of signal events.

The $Z(\rightarrow \nu\bar{\nu}) + 2j$ QCD background could be further reduced by taking advantage of its different color structure compared to the signal process. An important feature of WBF is the absence of color exchange between the two forward tagging jets, which results in less hadronic activity in the rapidity region between these jets [32]. Thus, vetoing additional soft jets in the central region could significantly reduce the QCD background while preserving most of the WBF signal. In Refs. [13] and [33], it is claimed that such a veto improves the signal-to-background ratio by a factor of three at the LHC. If a similar background reduction could be achieved at the Tevatron, the prospects for h_{inv} observation in the WBF channel would improve considerably: a 3σ observation in the WBF channel alone would then be possible with 6 fb^{-1} per detector, with a signal-to-background ratio close to $1/5$.

It is also important to consider the background normalization. In particular, to better understand the \cancel{p}_T distribution of the $Z(\rightarrow \nu\bar{\nu}) + 2j$ backgrounds, one may be able to make use of the channel $Z(\rightarrow \ell^+\ell^-) + 2j$ with the p_T of the Z boson reconstructed from the momenta of the two jets (to duplicate the systematic uncertainties of the \cancel{p}_T reconstruction from two jets). The rate for $Z(\rightarrow \ell^+\ell^-) + 2j$ is smaller than that for $Z(\rightarrow \nu\bar{\nu}) + 2j$ by about a factor of three due to the relative branching fractions of Z into $ee + \mu\mu$ versus neutrinos, so the statistics for this measurement will be limited. Nevertheless, one can imagine performing a fit or even a subtraction of the $Z(\rightarrow \nu\bar{\nu}) + 2j$ backgrounds.

IV. THE $h_{inv} + j$ SIGNAL

The $h_{inv} + j$ signal comes predominantly from Higgs production via gluon fusion, with one radiated jet. This is the dominant Higgs production channel at the Tevatron and the LHC and therefore merits attention in our study. The production cross section for $h + j$ at a hadron collider was first calculated in Ref. [34]. The cross sections were later given for the LHC and the Tevatron in Ref. [17]. The total signal cross sections are approximately 12 pb at the LHC and 0.1 pb at the Tevatron for $p_T(j) > 30 \text{ GeV}$ and $|\eta(j)| < 2.5$ [17]. We calculated the irreducible background for this process from $Z(\rightarrow \nu\bar{\nu}) + j$ for both LHC and Tevatron using Madgraph [18]. The cross section for this background is $\sim 1.5 \times 10^5 \text{ pb}$ at the LHC and $\sim 300 \text{ pb}$ at the Tevatron. We see that the number of background events is

larger than that of the signal by a factor of $10^3 - 10^4$. The only handles potentially available to distinguish signal from background are the p_T and rapidity of the jet. However, these distributions are similar for the signal and the background, so that significant reduction of the background is not possible while preserving most of the signal. In fact, a mono-jet plus \cancel{p}_T due to mis-measurement of the jets can be very substantial, and even impossible to overcome. Therefore, despite the large signal production rate, $h_{inv} + j$ is not a good channel for the discovery of an invisible Higgs.

V. DISCUSSION AND CONCLUSIONS

We studied the signals and backgrounds for an invisibly-decaying Higgs boson, h_{inv} , at present and future hadron colliders. Such an h_{inv} is motivated by the extremely narrow widths of the SM decay channels of a Higgs boson below the W pair threshold and the possible existence of light invisible particles (e.g., dark matter particles or quasistable singlets) beyond the SM to which the Higgs can decay. For example, in simple models where the dark matter particle is a real scalar, the mass of this scalar can be as low as ~ 5 GeV with $\mathcal{O}(1)$ couplings to the Higgs and $m_h < 150$ GeV [6, 7]. In the MSSM, an invisible Higgs can arise if h decays predominantly to a pair of lightest neutralinos¹ or via operators involving goldstinos permitted in non-linearly realized supersymmetry [36].

In this paper, we have assumed SM production rates for h_{inv} and a 100% invisible branching fraction. Our results can easily be rescaled for non-SM Higgs production rates and partly-visible decay branching fractions. The signal rate is simply scaled by the production rate and invisible branching fraction:

$$S = S_0 \frac{\sigma}{\sigma_{SM}} \frac{\text{BR}_{inv}}{1}, \quad (13)$$

where S_0 is the signal rate from our studies, σ/σ_{SM} is the ratio of the nonstandard production cross section to that of the SM Higgs, and BR_{inv} is the invisible branching fraction. Assuming that the SM is the only source of background, the luminosity required for a given signal

¹ While a light enough neutralino is disfavored in minimal supergravity due to the chargino mass bound from LEP II and the assumption of gaugino mass unification, an invisibly-decaying h is a definite possibility in a more general MSSM and in extensions of the MSSM containing additional electroweak-singlet chiral multiplets [35].

significance then scales like

$$\mathcal{L} = \mathcal{L}_0 \left[\frac{\sigma}{\sigma_{SM}} \frac{\text{BR}_{inv}}{1} \right]^{-2}, \quad (14)$$

where \mathcal{L}_0 is the luminosity required for a given significance found in our studies.

The prospects for the detection of h_{inv} at the LHC [11, 14] and the Tevatron [12] in the $Z + h_{inv}$ production channel have been studied before. We revisited $Z + h_{inv}$ production at the LHC, including new backgrounds not considered in Ref. [11] and modifying the kinematic cuts. Our results are in good agreement with those of Ref. [14]. The WBF production of h_{inv} at the LHC has been studied in Ref. [13]. We examined this channel at the Tevatron and established the kinematic cuts that are required to detect the WBF signal events. We found that this signal is crucial in making the observation of h_{inv} a possibility at the Tevatron. We also considered $h_{inv} + j$ production via gluon fusion at both the Tevatron and LHC.

The $Z + h_{inv}$ channel at the LHC can provide a h_{inv} discovery with only 10 fb^{-1} for $m_h = 120 \text{ GeV}$. With 30 fb^{-1} , discovery can be pushed out to $m_h = 160 \text{ GeV}$. This channel can be used at low m_h to supplement the previously-studied WBF channel, which has higher significance; it provides a second discovery channel with very different experimental systematics to confirm a discovery of h_{inv} in the WBF channel. The event rates in the $Z + h_{inv}$ and WBF channels could also be used to extract the Higgs boson mass from the production cross sections. Because the $Z + h_{inv}$ cross section falls faster with increasing m_h , it provides more sensitivity than WBF to m_h for $m_h \lesssim 160 \text{ GeV}$ once systematic uncertainties are included. Taking the ratio of rates in $Z + h_{inv}$ and WBF removes dependence on the production cross section and invisible decay branching fraction, allowing a more model-independent determination of the Higgs mass, with an uncertainty of 35–50 GeV (15–20 GeV) with 10 (100) fb^{-1} of integrated luminosity. The \cancel{p}_T distribution is also sensitive to m_h : larger m_h results in a larger average \cancel{p}_T in $Z + h_{inv}$ events. At the LHC, the production cross section and \cancel{p}_T distribution may be the only experimental handles on the mass of a Higgs boson with no visible decays.

By itself, h_{inv} production via WBF at the Tevatron provides a less than 2σ signal even with 10 fb^{-1} of integrated luminosity. However, combining this channel with $Z + h_{inv}$, studied previously, and combining the data from the two detectors gives the possibility of a 3σ observation of a 120 GeV h_{inv} with 7 fb^{-1} of delivered luminosity. This puts the observation of an invisibly-decaying Higgs boson within the realm of possibility at the Tevatron before data from the LHC is available. Vetoing additional soft jets in the central region could

significantly improve the observability of this channel.

Finally, we observe that $h_{inv} + j$ production via gluon fusion does not provide a useful signal at either the Tevatron or LHC. This is because there are not enough handles to separate the signal from the overwhelming background.

Acknowledgments

We thank V. Barger, J. Conway, I. Iashvili, F. Petriello, and A. Turcot for discussions, and R. Godbole for pointing out Ref. [14]. This work was supported in part by the U.S. Department of Energy under grant DE-FG02-95ER40896 and in part by the Wisconsin Alumni Research Foundation. The research of H.D. is also supported in part by the P.A.M. Dirac Fellowship, awarded by the Department of Physics at the University of Wisconsin-Madison. T.H. is also supported in part by a Fermilab Frontier Fellowship. Fermilab is operated by the Universities Research Association Inc. under Contract No. DE-AC02-76CH03000 with the U.S. Department of Energy.

-
- [1] R. Barate *et al.* [ALEPH Collaboration], Phys. Lett. B **565**, 61 (2003) [arXiv:hep-ex/0306033].
 - [2] M. W. Grünewald, arXiv:hep-ex/0304023; updated as:
S. Roth, talk given at “Rencontres de Moriond: QCD and Hadronic interactions”, La Thuile (Italy) , March 28 - April 4 2004, see:
moriond.in2p3.fr/QCD/2004/ThursdayAfternoon/Roth.pdf;
see also: lepewwg.web.cern.ch/LEPEWWG/Welcome.html.
 - [3] N. Arkani-Hamed, S. Dimopoulos, G. R. Dvali and J. March-Russell, Phys. Rev. D **65**, 024032 (2002) [arXiv:hep-ph/9811448].
 - [4] A. S. Joshipura and S. D. Rindani, Phys. Rev. Lett. **69**, 3269 (1992); A. S. Joshipura and J. W. F. Valle, Nucl. Phys. B **397**, 105 (1993).
 - [5] J. McDonald, Phys. Rev. D **50**, 3637 (1994).
 - [6] C. P. Burgess, M. Pospelov and T. ter Veldhuis, Nucl. Phys. B **619**, 709 (2001) [arXiv:hep-ph/0011335].
 - [7] H. Davoudiasl, R. Kitano, T. Li and H. Murayama, arXiv:hep-ph/0405097.

- [8] M. I. Josa [ALEPH, DELPHI, L3 and OPAL Collaborations], *Prepared for International Euro-physics Conference on High-Energy Physics (HEP 2001), Budapest, Hungary, 12-18 Jul 2001*, see: jhep.sissa.it/archive/prhep/preproceeding/007/145/higgs.pdf.
- [9] J. F. Gunion, Phys. Rev. Lett. **72**, 199 (1994) [arXiv:hep-ph/9309216]; B. P. Kersevan, M. Malawski and E. Richter-Was, Eur. Phys. J. C **29**, 541 (2003) [arXiv:hep-ph/0207014].
- [10] D. Choudhury and D. P. Roy, Phys. Lett. B **322** (1994) 368 [arXiv:hep-ph/9312347].
- [11] S. G. Frederiksen, N. Johnson, G. L. Kane and J. Reid, Phys. Rev. D **50**, 4244 (1994).
- [12] S. P. Martin and J. D. Wells, Phys. Rev. D **60**, 035006 (1999) [arXiv:hep-ph/9903259].
- [13] O. J. P. Eboli and D. Zeppenfeld, Phys. Lett. B **495**, 147 (2000) [arXiv:hep-ph/0009158].
- [14] R. M. Godbole, M. Guchait, K. Mazumdar, S. Moretti and D. P. Roy, Phys. Lett. B **571**, 184 (2003) [arXiv:hep-ph/0304137].
- [15] M. Battaglia, D. Dominici, J. F. Gunion and J. D. Wells, arXiv:hep-ph/0402062.
- [16] K. Belotsky, V. A. Khoze, A. D. Martin and M. G. Ryskin, Eur. Phys. J. C **36**, 503 (2004) [arXiv:hep-ph/0406037].
- [17] B. Field, S. Dawson and J. Smith, Phys. Rev. D **69**, 074013 (2004) [arXiv:hep-ph/0311199].
- [18] T. Stelzer and W. F. Long, Comput. Phys. Commun. **81**, 357 (1994) [arXiv:hep-ph/9401258]; F. Maltoni and T. Stelzer, JHEP **0302**, 027 (2003) [arXiv:hep-ph/0208156].
- [19] ATLAS-TDR, CERN-LHCC-99-014.
- [20] CMS-TDR, CERN-LHCC-97-31.
- [21] T. Han and S. Willenbrock, Phys. Lett. B **273**, 167 (1991); O. Brein, A. Djouadi and R. Harlander, Phys. Lett. B **579**, 149 (2004) [arXiv:hep-ph/0307206].
- [22] J. Ohnemus and J. F. Owens, Phys. Rev. D **43**, 3626 (1991); J. M. Campbell and R. K. Ellis, Phys. Rev. D **60**, 113006 (1999) [arXiv:hep-ph/9905386].
- [23] For a recent summary, see O. Brein, M. Ciccolini, S. Dittmaier, A. Djouadi, R. Harlander and M. Kramer, arXiv:hep-ph/0402003.
- [24] See, e.g., M. Dürrssen, ATL-PHYS-2003-030, available from <http://cdsweb.cern.ch>.
- [25] T. Figy, C. Oleari and D. Zeppenfeld, Phys. Rev. D **68**, 073005 (2003) [arXiv:hep-ph/0306109]; E. L. Berger and J. Campbell, Phys. Rev. D **70**, 073011 (2004) [arXiv:hep-ph/0403194].
- [26] D. L. Rainwater and D. Zeppenfeld, JHEP **9712**, 005 (1997) [arXiv:hep-ph/9712271].
- [27] D. L. Rainwater, D. Zeppenfeld and K. Hagiwara, Phys. Rev. D **59**, 014037 (1999) [arXiv:hep-ph/9808468].

- [28] T. Plehn, D. L. Rainwater and D. Zeppenfeld, Phys. Rev. Lett. **88**, 051801 (2002) [arXiv:hep-ph/0105325].
- [29] DØ Collaboration, DØNote-4366-CONF (2004).
- [30] D. Acosta *et al.* [CDF Collaboration], arXiv:hep-ex/0411059.
- [31] D. Acosta *et al.* [CDF Collaboration], arXiv:hep-ex/0410076.
- [32] V. D. Barger, R. J. N. Phillips and D. Zeppenfeld, Phys. Lett. B **346**, 106 (1995) [arXiv:hep-ph/9412276].
- [33] D. L. Rainwater, Ph.D. Thesis, arXiv:hep-ph/9908378.
- [34] R. K. Ellis, I. Hinchliffe, M. Soldate and J. J. van der Bij, Nucl. Phys. B **297**, 221 (1988).
- [35] T. Han, P. Langacker and B. McElrath, arXiv:hep-ph/0405244; A. Menon, D. E. Morrissey and C. E. M. Wagner, Phys. Rev. D **70**, 035005 (2004) [arXiv:hep-ph/0404184].
- [36] I. Antoniadis, M. Tuckmantel and F. Zwirner, arXiv:hep-ph/0410165.